



Pilot-scale biomethanation of cattle manure using dense membranes

Aline Lebranchu, Fabrice Blanchard, Michel Fick, Stéphane Pacaud, Eric Olmos, Stéphane Delaunay

► To cite this version:

Aline Lebranchu, Fabrice Blanchard, Michel Fick, Stéphane Pacaud, Eric Olmos, et al.. Pilot-scale biomethanation of cattle manure using dense membranes. Bioresource Technology, 2019, 284, pp.430-436. <10.1016/j.biortech.2019.03.140>. <hal-02968858>

HAL Id: hal-02968858

<https://hal.science/hal-02968858v1>

Submitted on 22 Oct 2021

HAL is a multi-disciplinary open access archive for the deposit and dissemination of scientific research documents, whether they are published or not. The documents may come from teaching and research institutions in France or abroad, or from public or private research centers.

L'archive ouverte pluridisciplinaire **HAL**, est destinée au dépôt et à la diffusion de documents scientifiques de niveau recherche, publiés ou non, émanant des établissements d'enseignement et de recherche français ou étrangers, des laboratoires publics ou privés.



Distributed under a Creative Commons CC BY-NC 4.0 - Attribution - Non-commercial use - International License

Pilot-scale biomethanation of cattle manure using dense membranes

Aline LEBRANCHU^{a,b}, Fabrice BLANCHARD^{a,b}, Michel FICK^{a,b}, Stéphane PACAUD^c, Eric OLMOS^{a,b,*}, Stéphane DELAUNAY^{a,b}

^a *CNRS, Laboratoire Réactions et Génie des Procédés, UMR 7274, 2 avenue de la forêt de Haye, TSA 40602, Vandœuvre-lès-Nancy, F-54518, France*

^b *Université de Lorraine, LRGP, UMR 7274, 2 avenue de la forêt de Haye, TSA 40602, Vandœuvre-lès-Nancy, F-54518, France*

^c *ENSAIA, Université de Lorraine, 2 avenue de la forêt de Haye, TSA 40602, Vandœuvre-lès-Nancy, F-54518, France.*

Abstract

This study aimed at studying the biomethanation process using a 100 L pilot-scale digester equipped with a dense membrane for hydrogen injection. Hydrogen mass transfer was characterized and the impact of hydrogen flowrate, agitation rate and of the co-injection of CO₂, on biogas production and composition, was precisely studied. A linear relationship between H₂ flowrate and the CO₂ and CH₄ rates in biogas was found but no impact on biogas flowrate was shown. It was also noticed that, without exogenous CO₂ injection, and for high H₂ injection flowrates, residual H₂ could be found at the digester outlet due to local CO₂ limitation. Thus, this study suggested that biogas production in biomethanation process at the pilot scale was probably rather limited by the dissolved CO₂ transport within the liquid phase than by the hydrogen mass transfer itself.

Keywords: biomethanation, permeation membrane, pilot-scale digester, methanization

*Corresponding author : eric.olmos@univ-lorraine.fr

1. Introduction

Anaerobic digestion is a natural biological process that transforms organic matter into biogas, consisting mainly of methane (about 60 %) and carbon dioxide (about 40 %). This is today a widespread way of producing green energies and that may simultaneously allow the recovery of organic wastes. To increase the rate of methane in the biogas, one possibility is the injection of hydrogen into the digesters. In fact, the natural production of hydrogen transformed into methane by hydrogenotrophic methanogenic *Archae* ($4\text{H}_2 + \text{CO}_2 \longrightarrow \text{CH}_4 + 2\text{H}_2\text{O}$) is limiting. Thus, by injecting exogenous hydrogen, the hydrogenotrophic methanogenic *Archae* could consume more CO_2 naturally produced in the reactor, and thus increase the rate of methane in biogas.

Injection of gaseous hydrogen to improve methanation reaction in digesters has been the subject of publications which demonstrated that several parameters may affect the efficiency of hydrogen injection, including the operating temperature and the mode of process performance. The main problem identified by Luo et al. (2012), Luo and Angelidaki (2012), Luo and Angelidaki (2013a) and Bassani et al. (2015) is indeed a problem of efficiency of hydrogen mass transfer in the reaction medium, leading to the presence of hydrogen in the biogas. These studies using different substrates (sludge STEP for Luo and Angelidaki (2012), bovine manure for Luo et al. (2012) and Luo and Angelidaki (2013a)) demonstrated the impact of some operating conditions on the effectiveness of the injection of hydrogen. These were the pressure of the H_2/CO_2 mixture injected in the headspace of the reactor (Luo et al., 2012), the agitation rate (Luo et al., 2012; Luo and Angelidaki, 2012, 2013a) and the design of the gas supplier (Luo and Angelidaki, 2012, 2013a).

Luo and Angelidaki (2012) also showed that the amount of dissolved hydrogen

26 was very small regarding the amount of hydrogen that was expected by applying a
27 mass balance on the gaseous hydrogen. With an injection of H_2 to 12 L/(L d) and
28 an agitation rate of 500 rpm, the dissolved concentration of H_2 was indeed about 8
29 $\mu\text{mol/L}$ while the expected one was 45 $\mu\text{mol/L}$. The difference between these two
30 values highlighted a limiting step of transfer from gas to liquid phase due to non-
31 adapted hydrodynamic conditions.

32 To improve the absorption of hydrogen in the liquid phase, two strategies were con-
33 sidered: the biogas recirculation and injection of hydrogen through membranes, in
34 order to avoid the formation of bubbles and the loss of H_2 in the outlet gas phase.
35 Biological methanation by recirculation of the biogas in the solution was proposed by
36 Alfaro et al. (2019) and Kougias et al. (2017). Three configurations of digesters and
37 different recirculation rates were compared by these last authors. Studied reactors
38 were two columns in series, a Continuous Stirred Tank Reactor and a bubble column.
39 The best results were achieved in the column reactors with the highest recirculation
40 and flowrate reaching a consumption of up to 100 % H_2 and in the bubble column,
41 with a rate of methane reaching 98 % in the biogas.

42

43 In order to address the problem of hydrogen absorption, in several studies, pure
44 hydrogen or hydrogen mixed with CO or CO_2 was injected by using permeation
45 hollow fiber membranes. The membranes used were non-porous polyurethane mem-
46 branes (Luo and Angelidaki, 2013b; Wang et al., 2013) or PVDF (polyvinylidene
47 fluoride) (Díaz et al., 2015). Studies using non-porous membranes agreed on the fact
48 that hydrogen was entirely consumed, since there was no hydrogen in the biogas.
49 Methane rates above 96 % in biogas were reported (Ju et al., 2008; Luo and Angel-
50 idaki, 2013b) which illustrated the effectiveness of an injection by permeation. The
51 study of Díaz et al. (2015) also showed a very good efficiency in the consumption of

hydrogen, with more than 95 % of the H_2 injected effectively consumed. However, it was found in this last study that, on the first days of digestion, a large part of the injected hydrogen was used for biomass growth, and not for the production of methane. Moreover, the development of a biofilm on the surface of the membrane was observed (Luo and Angelidaki, 2013b) and could increase the resistance of hydrogen mass transfer. Apart from the study of Kim et al. (2013), carried out in a 100 L reactor and considering an *ex-situ* culture of hydrogenotrophic *Archae*, the studies were conducted in low volumes laboratory-scale reactors.

In this study, biomethanation reaction was carried-out in a 100 L bioreactor, using a silicone permeation membrane, to assess the robustness of *in-situ* biomethanation at the pilot-scale. First, the permeation characteristics of the membrane and the gas-liquid mass transfer performance of this system were determined. Next, the impact of the shear rate and hydrogen flow rate on the biogas production and composition were studied. Finally, the performance of methanation were determined using a co-injection of hydrogen and CO_2 .

2. Materials and methods

2.1. Pilot-scale digester

The total volume of the tank was 142 L, with a diameter of $D_{vessel} = 500$ mm and a height $H = 760$ mm. The sketch of the bioreactor is reported on Figure 1. As demonstrated in a previous study (Lebranchu et al., 2017), the stirrer preferred was a double helical ribbon as it offered better mixing performance and allowed enhanced biogas productivity. This stirrer was combined here with a central Archimede's screw wrapped around the axis of agitation. Both systems were connected to an ATEX motor. The ribbon was sized in geometric similarity with the one previously used in

76 a 2 L digester as reported by Lebranchu et al. (2017). The pitch of the ribbon was
 77 500 mm, its width was 48 mm while its internal and external diameters were 384
 78 and 80 mm respectively. For the screw, the dimensions were a pitch of 298 mm, a
 79 blade width of 54 mm and an internal radius of 12 mm. The wrapping direction was
 80 opposite to that of the external ribbon. The agitator was also equipped with a Teflon
 81 scraper with a height of 35 mm to prevent the formation of crust at the bottom of
 82 the reactor. The control of the temperature at 40 °C was ensured by a double-heated
 83 jacket. The agitation rate varied, depending on the operating conditions used, as
 84 detailed in the results section. The digester operated in continuous-mode with a
 85 mean residence time of 28 days, which implied the supply of 3.5 L of cattle manure
 86 and removal of 3.5 L of digestate each day. Due to the viscosity of the liquid phase,
 87 two Archimede’s screw pumps (Air et Eau systèmes, Ludres, France) were used for
 88 supply and outlet. The supply was preliminary filtered using a grid with 6 mm
 89 diameter holes to prevent pipe plugging. Biogas composition and production were
 90 determined using dedicated on-line gas chromatography and gasmeter as previously
 91 described in Lebranchu et al. (2017).

92 *2.2. Dense membrane properties and characterization*

93 To avoid the presence of hydrogen in the biogas at the outlet of the reactor, which
 94 would require the introduction of a recirculation loop of the biogas, the hydrogen
 95 injection was not carried out by a conventional sparger but by permeation into a
 96 silicone tube pressurized by closing it at one end and wrapped around a cylindrical
 97 support. The silicone tube used was a membrane with 0.3 mm thickness and an
 98 internal diameter of 2 mm (Witeg, Wertheim, Germany). The permeability \mathcal{P} of the
 99 hydrogen in the silicone was obtained from equation 1 by applying various pressure
 100 gradients and measuring the related gas flow rate. The experiments were conducted

101 in air, water and digestate.

$$\mathcal{P} = \frac{Q \cdot e}{A \cdot \Delta P} \quad (1)$$

102 with \mathcal{P} ($\text{m}^3 \text{ m}/(\text{s m}^2 \text{ Pa})$) the membrane permeability, Q the volumetric flow rate
103 (m^3/s), e the membrane thickness (m), A the membrane surface (m^2) and ΔP (Pa)
104 the pressure difference. In order to enhance liquid circulation in the core of the vessel,
105 the diameter of the membrane support was increased to a maximal value of 324 mm.
106 A gap of 65 mm was left between the top of the scraper placed on the stirrer and the
107 bottom of the wrapping of the membrane tube to allow the circulation of the fluid.
108 For the same reason, a gap of 65 mm was applied between the top of the membrane
109 tube and the surface of the liquid. Using these conditions, a maximum of 100 m of
110 membrane could be wrapped. According to the equation 1, the expected hydrogen
111 flow rate **should** be 35 mL/min approximately.

112 The hydrogen flow rates and the volumetric gas-liquid mass transfer coefficients
113 $k_L a$ of the set-up were also determined. Gas-liquid mass transfer measurements
114 were carried-out by setting the permeation rate at the inlet of the membrane and
115 measuring the pressure inside the membrane tube. Dissolved H_2 was obtained from
116 the mass balance between the inlet and the outlet. The experiment was carried-out
117 as follows : The reactor was filled with 100 L of water heated gradually to 40 °C for
118 12 hours. Before the start of the measurements, a purge of the membrane tube was
119 done at 20 mL / min of H_2 for 20 min in order to remove the gases that could be
120 introduced inside the tube. The end of the tube was then closed and the flow rate
121 studied was fixed to the flow meter. Continuous hydrogen injections were made in
122 water at 10, 30 and 50 mL / min and, by the plot of equation 2, $k_L a$ (s^{-1}) value was
123 then obtained.

$$\ln \left(\frac{[H_2]^*}{[H_2]^* - [H_2]} \right) = k_L a \cdot t \quad (2)$$

with $[H_2]^*$ the concentration of H_2 at saturation, $[H_2]$ the concentration of H_2 in the solution and t the time (s).

3. Results and discussion

3.1. Gas-liquid mass transfer

The permeability of hydrogen in the silicone was determined at 40°C using several injection rates (30, 50 and 70 mL / min) and considering permeation in air to neglect the resistance of mass transfer in the fluid phase (Figure 2). A value of $\mathcal{P} = 7.33 \times 10^{-14}$ (m³ m) / (s m² Pa) was obtained. As expected, the increase of the resistance of mass transfer entailed a slower permeation of hydrogen in water and in digestate due to the significant increase of the resistance to mass transfer when air is replaced by these two fluids (Figure 2). In parallel, the determination of $k_L a$ values, carried-out at a agitation rate of 10 rpm (namely for a constant power dissipation per unit of volume) provided values of approximately 1 h⁻¹ (Figure 2). No study determining the value of $k_L a$ of a dense membrane for hydrogen injection in digesters have been carried out at the pilot-scale making hard the comparison of **the present** values with literature data. An increase of the agitation rate to 40 rpm did not promote an increase in the hydrogen absorption rate as H_2 microbubbles, formed and attached to the membrane, detached then due to higher local shear stress, causing a sudden release of gaseous H_2 and then a decrease in the amount of dissolved hydrogen.

3.2. Validation of pilot-scale digester

The biogas flowrate profile showed that, after 17 days of production, it reached an asymptotic value of about 5.2 NL/h (or 1 NL/(h kg_{OM})), which corresponded to

146 a production of 125 L of biogas per day. Considering the daily addition of 3.5 L of
 147 liquid cattle manure, at a rate of about 11 % of organic matter, biogas production
 148 was approximately 324 L/kg_{OM}. This result was thus in agreement with the expected
 149 values of biogas production using cattle manure (Teixeira Franco et al., 2017). The
 150 initial pH was 7.9, corresponding to the pH of the digestate used for initial reactor
 151 filling. During the first 7 days of digestion, a slight pH decrease was observed before
 152 a stabilization to 7.5 after 20 days of digestion, which corresponded to range of values
 153 of 7.5 to 8, typically encountered in digesters (Bassani et al., 2015).
 154 The analysis of biogas composition revealed a maximal methane content of 63.6 %
 155 and a minimal CO₂ rate of 36.3 % after 3 days of digestion. This initial process
 156 sequence, rather favourable to methane production was already noticed in differ-
 157 ent metagenomic studies such as the works of Montero et al. (2008) on a synthetic
 158 medium or of Chachkhiani et al. (2004) using liquid cattle manure. This suggested
 159 thus an initial production of CH₄ by the hydrogenotrophic *Archae* rather than by
 160 the acetotrophic populations leading to the reduction of CO₂. Biogas composition
 161 progressively stabilized after 7 days of digestion at rate values of 57.7 % for CH₄
 162 and 42 % for CO₂. The results obtained without hydrogen injection thus validated
 163 the pilot-scale digester as a scale-up of the equipment used by Lebranchu et al.
 164 (2017) for cattle manure methanization and could thus be used for further study of
 165 biomethanation process.

166 3.3. *In-situ biomethanation*

167 3.3.1. *Impact of H₂ flowrate on biogas flowrate*

168 After each steady-state, H₂ flow rate was progressively increased from 12 to 31
 169 mL/min. Biogas flow rate per kg of organic matter was determined and given in Fig-
 170 ure 3A. Hydrogen injection, whatever the flowrate used, did not seem to significantly

171 modify biogas flowrate. This was previously observed by Luo et al. (2012) by increas-
 172 ing partial pressure of H_2 in a digester headspace. This result was also consistent
 173 with the bioreaction stoichiometry as one molecule of CO_2 should be transformed
 174 into one molecule of methane. This also meant that all injected hydrogen was ef-
 175 fectively consumed. As the consumption of exogenous H_2 led to the consumption
 176 of a fraction of the dissolved CO_2 , there was also a concomitant slight increase in
 177 the pH value after each increase of hydrogen flowrate (Figure 3B), from 7.5 to al-
 178 most 7.7 for H_2 flow rate of 31 mL/min. However, this increase, also observed in
 179 other studies of biological methanation (Szuhaj et al., 2016; Luo et al., 2012; Luo
 180 and Angelidaki, 2013a), remained weak and did not seem to significantly affect the
 181 production process as the flow rate of biogas remained overall constant (Figure 3A).

182 3.3.2. Impact of H_2 flowrate on biogas composition

183 On the contrary to biogas flow rate, CH_4 and CO_2 biogas contents significantly
 184 depended on the H_2 flowrate as indicated by the measurements reported in Figure
 185 3A. A progressive decrease in CO_2 content and a corresponding increase in CH_4 con-
 186 tent were indeed observed when H_2 flowrate increased. Figure 3A also shows that, in
 187 the mean time, the time interval between change in H_2 flow rate and biogas content
 188 stabilization was reduced. Whereas five days were needed to achieve the stabiliza-
 189 tion after switching the H_2 flowrate from 0 to 12 mL/min, three days were indeed
 190 sufficient to achieve stability after the switch from 20 to 31 mL/min. This suggested
 191 a possible adaptation of microbial populations to the presence of H_2 , including the
 192 increase in the hydrogenotrophic bacteria population, promoting a reduction of the
 193 necessary stabilization time. Studies of Agneessens et al. (2017), Treu et al. (2018),
 194 and Alfaro et al. (2018, 2019) demonstrated by microbial community characterization
 195 that microbial populations were able to adapt to a H_2 injection but also that this

196 adaptation was strongly linked to the process operation parameters (modes of injection of H₂, flow rates, substrates, reactor scale). The relationships between CH₄ and
 197 CO₂ contents and injected H₂ flowrates were reported in Figure 4. Interestingly, the
 198 experimental measurements could be fitted using a linear model which was expected
 199 regarding reaction stoichiometry. Considering that the molar volume remained in-
 200 deed the same whatever the gas, a mole of CH₄ should be produced for each mole
 201 of CO₂ consumed. Knowing that the flow of biogas is 5.2 L/h, the slope obtained of
 202 0.35 corresponded to 0.3 mL/min of additional CH₄ for 1 mL/min H₂ added. How-
 203 ever, theoretically, with the addition of 1 mL/min of H₂, the CH₄ flowrate should
 204 be of 0.25 mL/min. This clearly confirmed the efficiency of conversion of hydro-
 205 gen into methane and that the injected hydrogen was completely consumed. This
 206 also suggested that consumed hydrogen seemed not significantly used for biomass
 207 growth, as Díaz et al. (2015) already showed. The total consumption of hydrogen
 208 was confirmed by the analysis of biogas with H₂ rates lower than 0.05 % (Figure
 209 3A) despite weak amounts of H₂ of approximately 0.04 % at an hydrogen flowrate
 210 of 31 mL/min were determined. The simultaneous presence of CO₂ at high volume
 211 fractions also seemed to indicate the occurrence of local H₂ saturations in the biore-
 212 actor inducing a release of gaseous hydrogen. This may be explained either (i) by a
 213 physical limitation, namely the injected hydrogen was not dispersed quickly enough
 214 in the reactor in comparison with the inlet flowrate of hydrogen, leading to local
 215 saturation and the appearance of a gas phase hydrogen or (ii) by a biological limi-
 216 tation, namely *Archae* were not locally able to consume all the amount of injected
 217 hydrogen or (iii) by a local limitation of CO₂ that stopped the H₂ consumption.
 218 Even if biogas recirculation is an interesting option to limit H₂ loss, further develop-
 219 ments regarding efficiency of 'one-pass' hydrogen injection, namely without biogas
 220 recirculation, should be intensified. Jensen et al. (2018) indeed demonstrated that
 221

222 it should remain the optimal solution from a mass transfer performance point of view.

223

224 3.4. Impact of shear stress on biogas production during biomethanation

225 As noted previously, when the hydrogen flow rate and the agitation rate were
226 respectively 31 mL/min and 10 rpm, traces of H₂ were measured at the outlet of
227 the reactor. Thus, the frequency of agitation was modified in order to improve the
228 distribution of hydrogen in the reactor and potentially to reduce this loss and to
229 increase the CH₄ rate. The study of the impact of agitation rate was therefore
230 performed here in the presence of an injection of H₂ to 31 mL/min.

231 3.4.1. Impact on biogas flowrate

232 The temporal evolution of the flowrate of biogas for different conditions of agita-
233 tion is presented in Figure 5. The increase in the agitation rate from 10 to 20 rpm
234 did not have a significant impact on the flowrate of biogas. However, the reduction
235 of agitation from 20 to 5 rpm led to an increase in the average flow rate from 0.89
236 to 1.14 L/(h kg_{OM}), but also to temporal fluctuations of this flow rate. This could
237 be related to the results of previous paper dealing with the impact of agitation on
238 the performance on biogas production in a 2 L digester (Lebranchu et al., 2017). It
239 was indeed shown that the increase in agitation from 10 to 50 and 90 rpm, led to a
240 reduction of the amount of biogas, probably due to the increase in the maximum in
241 shear stress the reactor and the resulting damage of microbial aggregates. As shown
242 by Lebranchu et al. (2017), this shear stress could be expressed by equation 3:

$$\sigma = K \cdot \dot{\gamma}^n \quad (3)$$

243 with K (Pa s^{*n*}) the consistency index and n () the flow index for the cattle manure
 244 digestate. Then the following equation may also be obtained:

$$\frac{\sigma_{max100L}}{\sigma_{max2L}} \propto \left(\frac{\dot{\gamma}_{max100L}}{\dot{\gamma}_{max2L}} \right)^n \quad (4)$$

245 with $\sigma_{max100L}$ and σ_{max2L} (Pa) and $\dot{\gamma}_{max100L}$ et $\dot{\gamma}_{max2L}$ the maximal shear stresses
 246 and maximal shear rates in both systems respectively. Assuming that maximal shear
 247 rate $\dot{\gamma}_{max}$ was encountered in the gap between the ribbon and the vessel wall, it could
 248 be estimated by equation 5.

$$\dot{\gamma}_{max} = \frac{\pi \cdot N \cdot D}{\frac{D_{vessel} - D}{2}} \quad (5)$$

249 with D_{vessel} the vessel diameter, D the external ribbon diameter and N the agitation
 250 rate. The width of the gap in the 100 L reactor was also decreased relatively to its
 251 length obtained theoretically by geometric similarity of the 2L reactor in order to
 252 increase the heat transfer and limit the formation of crust close to the outer wall.
 253 Thus, the maximal shear rate reached 12.6 s⁻¹ in 100 L reactor at 5 rpm, which is
 254 2 times higher than the one obtained in the 2 L reactor at 10 rpm (6.1 s⁻¹). The
 255 maximal shear stress obtained at 10 rpm in 2 L reactor was about 30 Pa (Lebranchu
 256 et al., 2017), so according to equation 4, the maximal shear stress obtained at 5 rpm
 257 in the pilot reactor was 37.2 Pa. Using the same method of calculation, the maximal
 258 shear stress at the pilot-scale and at an agitation rate of 10 rpm was then estimated
 259 at σ_{max} = 47 Pa. Thus, the maxim shear stress in 2 L at N = 10 rpm was similar
 260 to the one expected in the 100 L digester for N = 5 rpm, and matched the critical
 261 shear stress that should not be exceeded, as determined in Lebranchu et al. (2017).
 262 During the experiment at N = 10 rpm in the 100 L reactor, the maximal stress was

thus high enough to lead to a reduction of the biogas flowrate. Moreover, the variability of the flow rate was more important at an agitation rate of 5 rpm in comparison with 10 or 20 rpm agitations. This phenomenon found no explanation by the measurements and no high frequency fluctuations could be put into evidence. The change in the frequency of agitation did not significantly change the pH of the digestate (data not shown). The relative stability of the pH during this period indicated that the balance between the production and consumption of volatile fatty acids was globally not impacted by the agitation rate. The biogas flow variations observed at $N = 5$ rpm could therefore not be explained by pH fluctuations.

3.4.2. Impact on biogas composition

The evolution of the composition in CH_4 and CO_2 flowrates for the various agitation rates (10, 20 and 5 rpm) was reported in Figure 5. The increase in agitation from 10 to 20 rpm allowed an increase in CH_4 rate from 68.0 to 68.8 %, a decrease in CO_2 rate from 31.7 to 30.9 % and a residual H_2 rate reduction from 0.041 to 0.034 %. This suggested that a stronger agitation allowed a better homogeneity of the H_2 and thus a more efficient consumption. The change from $N = 20$ to 5 rpm led also to biogas composition fluctuations. This destabilization was accompanied by a decrease in the average CH_4 rate to 66.7 %, an increase in the CO_2 rate to 33.1 % and an increase in the H_2 rate to 0.08 %. Considering the respective flow rates of each gas component, a slight increase in hydrogen flow rate of 1 mL/h at 20 rpm versus 3 mL/h to 5 rpm, which seemed to indicate to a slight decline in methane flow rate, but CH_4 flow rate increased from 3.03 to 3.5 L/h. Thus, the hydrogen mass balance was not in total agreement with the one in methane, with a simultaneous increase in the flow of methane and hydrogen. These results suggested that the additional

methane produced was not related to the injection of hydrogen but could be the consequence of better syntrophic relationships between bacteria as it was already suggested in the study of Lebranchu et al. (2017). Thus, it was concluded that the increase in agitation allowed a better distribution of hydrogen in the reactor, promoted a reduction in H_2 rate in biogas, but also caused a decrease in overall biogas production flow. The agitation was then set back to 10 rpm for the rest of the study.

3.5. Addition of exogenous CO_2

To further validate the hypothesis of local CO_2 limitation, CO_2 was added in the injected gas, by applying the ratio of H_2 and total C carbon rates $H_2/C = 8.8$. This addition was carried-out in 2 steps. First, the addition of CO_2 was made at a flow rate of 3.5 mL/min, while maintaining the flow of H_2 at 31 mL/min. In a second step, the flow rate of CO_2 was maintained constant at 3.5 mL/min while H_2 flow rate was increased till total consumption of injected CO_2 . The Figure 6 reports the total flow rate of biogas at the outlet of the digester. A slight increase in this flow rate was observed throughout the period of CO_2 injection, from 5.0 L/h to 5.6 L/h. The observed increase of the overall flow rate was consistent with what was expected, although this increase was three times higher than the expected value for a CO_2 inlet flow rate of 0.21 L/h. Besides, no decrease of pH during the addition of CO_2 was observed meaning there was no accumulation of CO_2 in the reactor. This suggested that dissolved CO_2 remained close to the permeation membrane, and that it was either consumed, or accumulated before its stripping. This would suggest a local decrease of the pH, close to the membrane, as previously demonstrated by Garcia-Robledo et al. (2016). Lastly, the increase of H_2 flow rate led to a slight increase in the pH measured, from 7.7 to 7.8, which was consistent with the consumption of CO_2 naturally formed by the digestion process.

313

314 The injection of CO₂ at 3.5 mL/min with a H₂ flow rate of hydrogen set at 31
315 mL/min led to an increase in the rate of CO₂ in biogas and, consequently, a decrease
316 in CH₄ rate (Figure 6). Combined with the overall increase in the flow of biogas, this
317 increase in CO₂ rate led to the increase in CO₂ outflow from 1.66 to 1.94 L/h, while
318 CO₂ injected was 0.21 L/h, indicating an overproduction of CO₂ in these conditions.
319 Figure 6 shows that the amount of CO₂ consumed is not zero because the present rate
320 of H₂ in the biogas decreased in the presence of CO₂. Concerning H₂, its rate fell from
321 0.16 to 0.008 %, meaning its flow rate decreased from 0.13 to 0.0083 mL/min. At the
322 same time, methane rate was reduced from 66.7 to 65.1 %, but the increase in overall
323 throughput of biogas led to an increase in the overall rate of methane from 3.34 to
324 3.66 L/h. The increased flow rate of methane is qualitatively consistent with the
325 decrease in the rate of hydrogen. Quantitatively, the simultaneous overproduction of
326 CO₂ and CH₄ could be explained by the acetotrophic *Archae* that produce both of
327 CH₄ and CO₂. The local decrease in pH mentioned earlier would be the consequence
328 of the activity of the acetotrophic *Archae*. This phenomenon was demonstrated by
329 the study of Hao et al. (2013) who observed changes in bacterial populations during
330 changes of pH conditions. It has been highlighted that the increase in the pH above
331 7.5 led to an inhibition of the activity of the acetotrophic methanogenic *Archae* .
332 Thus, considering the initial pH of 7.8 in the whole of the reactor, the addition of
333 CO₂ could have led to a local decrease in pH below 7.5, which would cause the over-
334 production of methane and CO₂. Thus, it seems that, qualitatively, the depletion of
335 H₂ in the outlet gas was explained by consumption of a fraction of CO₂. However,
336 it remained difficult to quantify it more precisely due to the increased production of
337 CO₂ by acetotrophic *Archae* .
338 The addition of extra CO₂ mixed with the H₂ allowed the total consumption of

the H₂ (Figure 6). This could explain why hydrogen was detected in outlet biogas for flow injection of 31 mL/min of pure hydrogen, even if CO₂ was macroscopically available. The study of Garcia-Robledo et al. (2016) showed that injected H₂ and CO₂ consumption was carried out in a millimetric layer near the membrane. This suggested that, in the absence of CO₂ injected, the existence of residual hydrogen was due to a CO₂ limitation near the membrane. A realistic assumption is that the injected H₂ locally reacted with CO₂ which, once the latter fully consumed, caused a local accumulation of hydrogen beyond its solubility, entailing its stripping. So, there was probably a limitation of hydrogen transport from the membrane towards the rest of the reactor and a limitation on the transport of CO₂ from bulk to the membrane permeation vicinity. This assumption was also previously proposed by Garcia-Robledo et al. (2016) and Agneessens et al. (2018) in 1.4 L lab-scale digesters.

In order to consume the injected CO₂, H₂ flow rate was progressively increased while keeping constant the CO₂ flow rate to 3.5 mL/min. It should be noted that it was necessary to increase the H₂ flow rate up to 42 mL/min (Figure 6) to achieve a CO₂ rate in the biogas similar to the rate of CO₂ with pure H₂ injection, i.e. to consume all of the exogenous CO₂. Even if the increase in total production of biogas was explained by overproduction by the acetotrophic *Archae*, this consumption of additional hydrogen showed that the hydrogenotrophic *Archae* were always present and active. Flow rate of biogas was stable at 5.6 L/h over the period, but the flow rate of methane increased up to 3.8 L/h and that of CO₂ decreased to 1.8 L/h. The difference was thus + 0.14 L/h in CH₄ and - 0.14 L/h in CO₂. The surplus of added hydrogen was thus 0.66 L/h, while the theoretical value was 0.17 L/h of additional methane and 0.17 L/h for CO₂ consumption. The results obtained in the digester were therefore relatively close to the theoretical values. Throughout this period,

365 the injected H_2 was completely consumed, which confirmed the effectiveness of the
366 permeation membrane for the intensification of production as long as it remained
367 some CO_2 to consume in the membrane vicinity.
368 Lastly, the injection of CO_2 was shut-off, which led to the decrease in the flow of
369 biogas from 5.6 to 5.0 L/h (Figure 6), to the increase in CH_4 rate to 70.5 %, to
370 the decrease in CO_2 rate at 28.9 % and the measurement of about 0.4 % H_2 in the
371 biogas. The presence of hydrogen in the biogas while keeping a CO_2 rate of nearly 30
372 % indicated the appearance of a local saturation, likely located in the environment
373 of the membrane.

374 4. Conclusion

375 Biomethanation of cattle manure was validated in a 100 L digester using a dense
376 membrane for H_2 injection. This injection was shown to strongly limit the undis-
377 solved H_2 rate in the biogas produced. A linear relationship was found between the
378 CH_4 content in the biogas and the H_2 flowrate. The co-injection of exogenous CO_2
379 with H_2 revealed that biogas production was probably limited by the dissolved CO_2
380 transport within the liquid phase volume, which addresses the issue of the definition
381 of robust scale-up rules for biomethanation processes and for designs of gas injection
382 systems.

383 Acknowledgements

384 This work was supported by ADEME and Programme d'Investissements d'Avenir
385 (research program VALORCO).

386 References

- 387 1. Agneessens, L. M., Ottosen, L. D. M., Andersen, M., Olesen, C. B., Feilberg,
388 A., Kofoed, M. V. W., 2018. Parameters affecting acetate concentrations dur-
389 ing in-situ biological hydrogen methanation. *Bioresource Technol.* 258, 33-40.
- 390 2. Agneessens, L. M., Ottosen, L. D. M., Voigt, N. V., Nielsen, J. L., de Jonge, N.,
391 Fischer, C. H., Kofoed, M. V. W., 2017. In-situ biogas upgrading with pulse H₂
392 additions: The relevance of methanogen adaption and inorganic carbon level.
393 *Bioresource Technol.* 233, 256-263.
- 394 3. Alfaro, N., Fdz-Polanco, M., Fdz-Polanco, F., Diaz, I., 2018. Evaluation of
395 process performance, energy consumption and microbiota characterization in
396 a ceramic membrane bioreactor for ex-situ biomethanation of H₂ and CO₂.
397 *Bioresource Technol.* 258, 142-150.
- 398 4. Alfaro, N., Fdz-Polanco, M., Fdz-Polanco, F., Diaz, I., 2019. H₂ addition
399 through a submerged membrane for in-situ biogas upgrading in the anaerobic
400 digestion of sewage sludge. *Bioresource Technol.* 280, 1-8.
- 401 5. Bassani, I., Kougias, P. G., Treu, L., Angelidaki, I., 2015. Biogas upgrading via
402 hydrogenotrophic methanogenesis in two-stage continuous stirred tank reactors
403 at mesophilic and thermophilic conditions. *Environ. Sci. Technol.* 49, 12585-
404 12593.
- 405 6. Chachkhiani, M., Dabert, P., Abzianidze, T., Partskhaladze, G., Tsiklauri, L.,
406 Dudaui, T., Godon, J., 2004. 16s rDNA characterisation of bacterial and
407 archaeal communities during start-up of anaerobic thermophilic digestion of
408 cattle manure. *Bioresource Technol.* 93, 227-232.
- 409 7. Diaz, I., Perez, C., Alfaro, N., Fdz-Polanco, F., 2015. A feasibility study on the
410 bioconversion of CO₂ and H₂ to biomethane by gas sparging through polymeric

- 411 membranes. *Bioresource Technol.* 185, 246-253.
- 412 8. Garcia-Robledo, E., Ottosen, L. D., Voigt, N. V., Kofoed, M., Revsbech, N.
413 P., 2016. Micro-scale H₂-CO₂ dynamics in a hydrogenotrophic methanogenic
414 membrane reactor. *Frontiers in Microbiol.* 7, 1276.
- 415 9. Hao, L., Lu, F., Li, L., Wu, Q., Shao, L., He, P., 2013. Self-adaption of
416 methaneproducing communities to pH disturbance at different acetate concen-
417 trations by shifting pathways and population interaction. *Bioresource Technol.*
418 140, 319-327.
- 419 10. Jensen, M. B., Kofoed, M. V. W., Fischer, K., Voigt, N. V., Agneessens, L.
420 M., Batstone, D. J., Ottosen, L. D. M., 2018. Venturi-type injection system as
421 a potential H₂ mass transfer technology for full-scale in situ biomethanation.
422 *Appl. Energ.* 222, 840-846.
- 423 11. Ju, D.-H., Shin, J.-H., Lee, H.-K., Kong, S.-H., Kim, J.-I., Sang, B.-I., 2008. Ef-
424 fects of pH conditions on the biological conversion of carbon dioxide to methane
425 in a hollow-fiber membrane biofilm reactor (Hf-MBfR). *Desalination* 234, 409-
426 415.
- 427 12. Kim, S., Choi, K., Chung, J., 2013. Reduction in carbon dioxide and pro-
428 duction of methane by biological reaction in the electronics industry. *Int. J.*
429 *Hydrogen Energ.* 38, 3488-3496.
- 430 13. Kougiass, P. G., Treu, L., Benavente, D. P., Boe, K., Campanaro, S., Angeli-
431 daki, I., 2017. Ex-situ biogas upgrading and enhancement in different reactor
432 systems. *Bioresource Technol.* 225, 429-437.
- 433 14. Lebranchu, A., Delaunay, S., Marchal, P., Blanchard, F., Pacaud, S., Fick, M.,
434 Olmos, E., 2017. Impact of shear stress and impeller design on the production
435 of biogas in anaerobic digesters. *Bioresource Technol.* 245, 1139-1147.
- 436 15. Luo, G., Angelidaki, I., 2012. Integrated biogas upgrading and hydrogen uti-

- 437 lization in an anaerobic reactor containing enriched hydrogenotrophic methanogenic
438 culture. *Biotechnol. Bioeng.* 109, 2729-2736.
- 439 16. Luo, G., Angelidaki, I., 2013a. Co-digestion of manure and whey for in situ
440 biogas upgrading by the addition of H₂: Process performance and microbial
441 insights. *Applied Microbiol. Biot.* 97, 1373-1381.
- 442 17. Luo, G., Angelidaki, I., 2013b. Hollow -fiber membrane based H₂ diffusion for
443 efficient in situ biogas upgrading in an anaerobic reactor. *Appli. Microbiol.*
444 *Biot.* 97, 3739-3744.
- 445 18. Luo, G., Johansson, S., Boe, K., Xie, L., Zhou, Q., Angelidaki, I., 2012a.
446 Simultaneous hydrogen utilization and in situ biogas upgrading in an anaerobic
447 reactor. *Biotechnol. Bioeng.* 109, 1088-1094.
- 448 19. Luo, G., Johansson, S., Boe, K., Xie, L., Zhou, Q., Angelidaki, I., 2012b.
449 Simultaneous hydrogen utilization and in situ biogas upgrading in an anaerobic
450 reactor. *Biotechnol. Bioeng.* 109, 1088-1094.
- 451 20. Montero, B., Garcia-Morales, J., Sales, D., Solera, R., 2008. Evolution of
452 microorganisms in thermophilic-dry anaerobic digestion. *Bioresource Technol.*
453 99, 3233-3243.
- 454 21. Szuhaj, M., Acs, N., Tengolics, R., Bodor, A., Rakhely, G., Kovacs, K. L.,
455 Bagi, Z., 2016. Conversion of H₂ and CO₂ to CH₄ and acetate in fed-batch
456 biogas reactors by mixed biogas community: a novel route for the power-to-gas
457 concept. *Biotechnol. Biofuels* 9, 102.
- 458 22. Texeira Franco, R., Buffiere, P., Bayard, R., 2017. Cattle manure for biogas
459 production. Does ensiling and wheat straw addition enhance preservation of
460 biomass and methane potential? *Biofuels*, 1-12.
- 461 23. Treu, L., Kougias, P. G., de Diego-Diaz, B., Campanaro, S., Bassani, I.,
462 Fernandez-Rodriguez, J., and Angelidaki, I. 2018. Two-year microbial adap-

- 463 tation during hydrogen-mediated biogas upgrading process in a serial reactor
464 configuration. *Bioresource Technol.* 264, 140-147.
- 465 24. Wang, W., Xie, L., Luo, G., Zhou, Q., Angelidaki, I., 2013. Performance
466 and microbial community analysis of the anaerobic reactor with coke oven gas
467 biomethanation and in situ biogas upgrading. *Bioresource Technol.* 146, 234-
468 239.

469 **Figure captions**

470 **Figure 1.** Sketch of the bioreactor used in the present study.

471

472 **Figure 2.** Impact of transmembrane pressure on hydrogen permeation flow rate
473 in the case of permeation in air (■), in water (▲) and in digestate (●) and on the
474 volumetric gas-liquid mass transfer coefficient k_La in digestate (×).

475

476 **Figure 3.** (A) Temporal profile of biogas flowrate (□) and composition in CO₂
477 (◇), H₂ (*) and CH₄ (○) and (B) pH.

478

479 **Figure 4.** Impact of H₂ flowrate on the rates of methane (○) and CO₂ (◇).

480

481 **Figure 5.** Impact of agitation rate on the total (□), CO₂ (◇), H₂ (*) and CH₄
482 (○) volumetric flowrates.

483

484 **Figure 6.** Impact of CO₂+H₂ injection on the CO₂ (◇), H₂ (*) and CH₄ (○) biogas
485 composition and total biogas volumetric flowrate (□) .

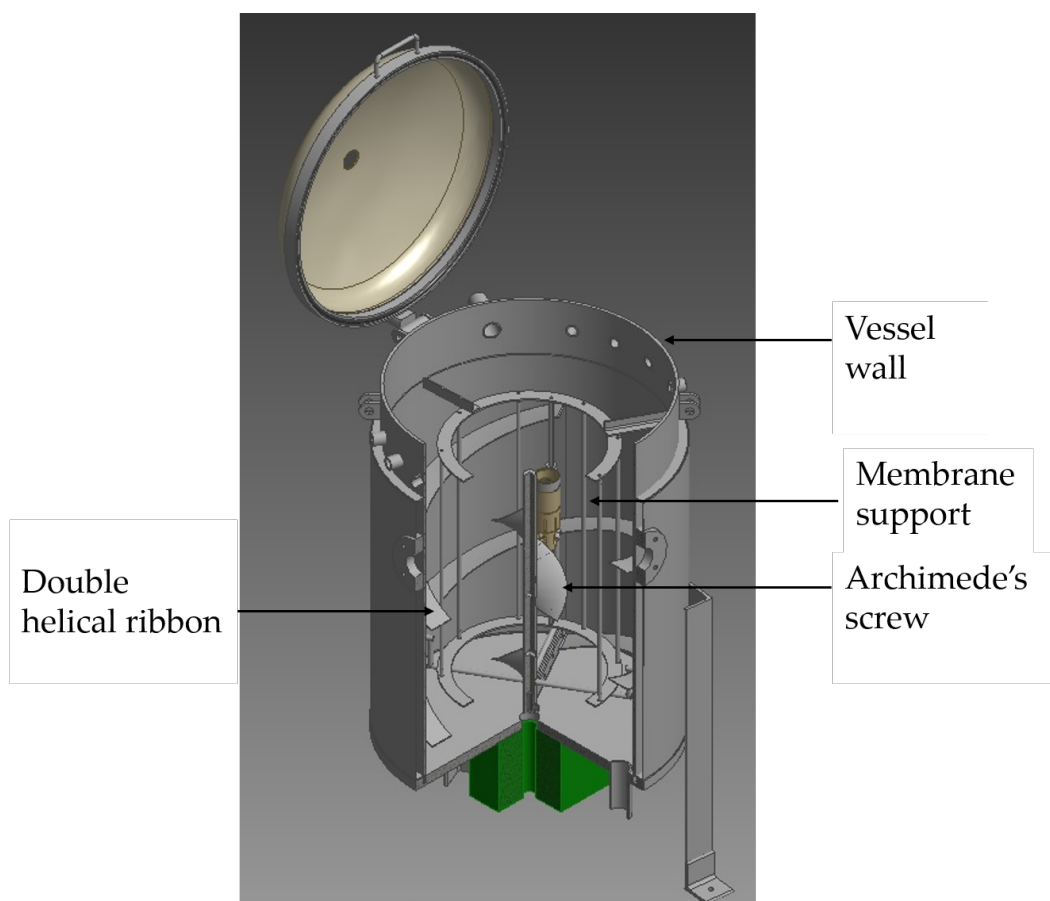


Figure 1: Sketch of the bioreactor used in the present study.

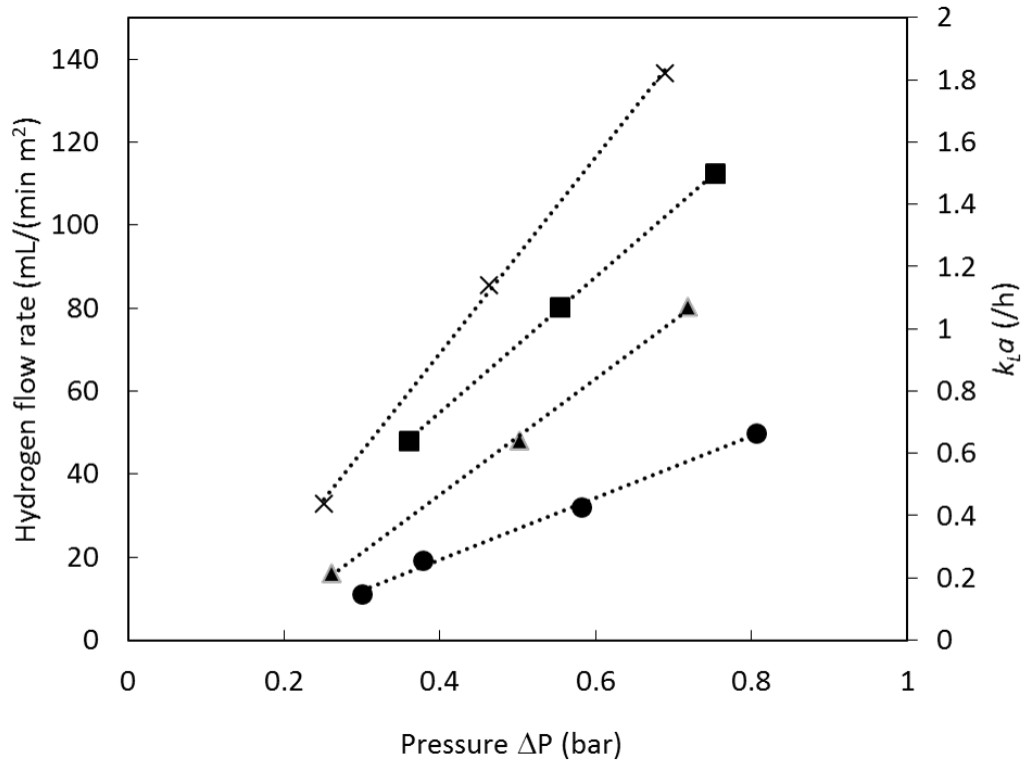
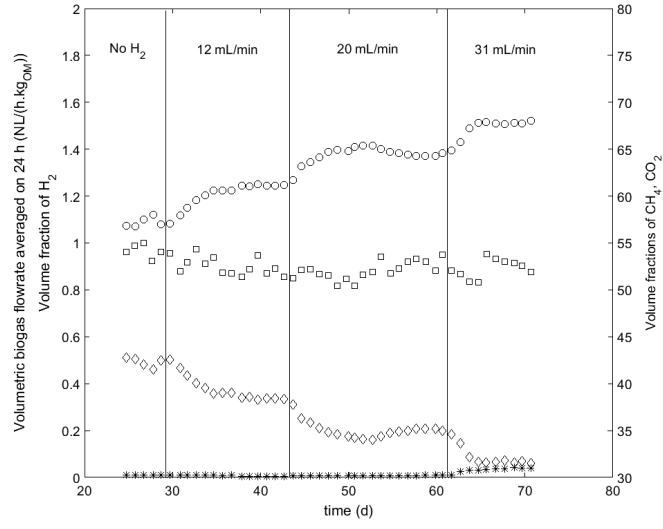
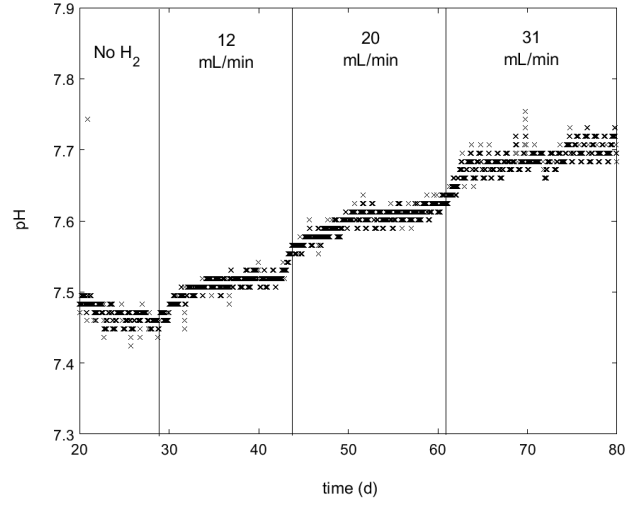


Figure 2: Impact of transmembrane pressure on hydrogen permeation flow rate in the case of permeation in air (■), in water (▲) and in digestate (●) and on the volumetric gas-liquid mass transfer coefficient k_{La} in digestate (×.)



(A)



(B)

Figure 3: (A) Temporal profile of biogas flowrate (\square) and composition in CO₂ (\diamond), H₂ (*) and CH₄ (\circ) and (B) pH.

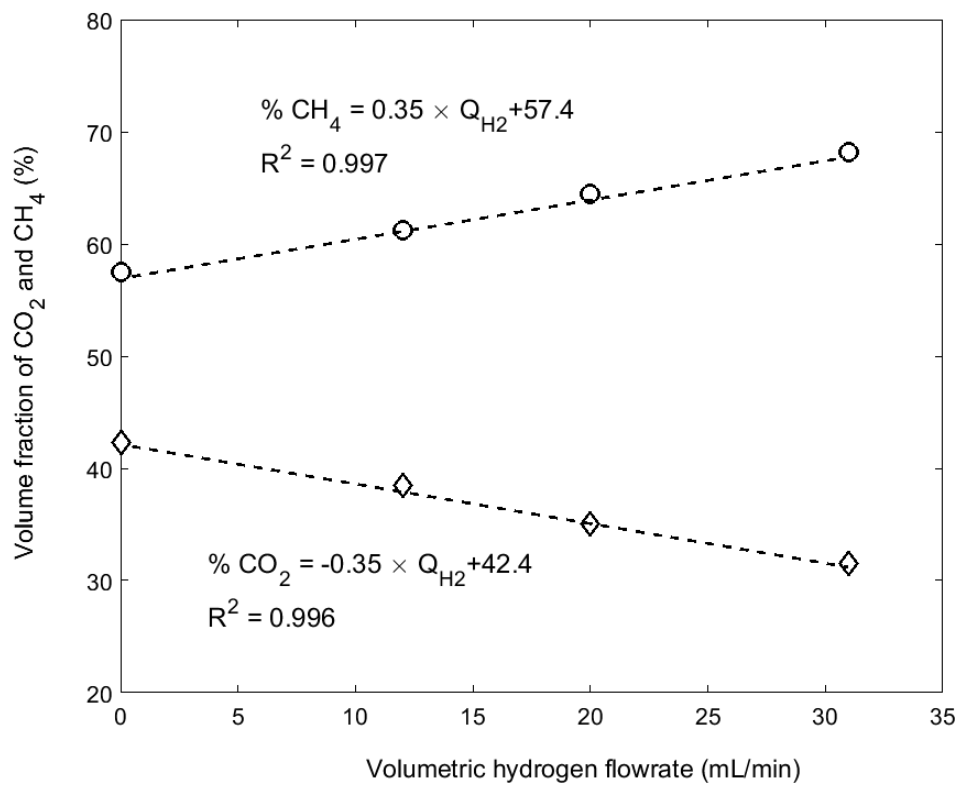


Figure 4: Impact of H₂ flowrate on the rates of methane in CO₂ (◇) and CH₄ (○) .

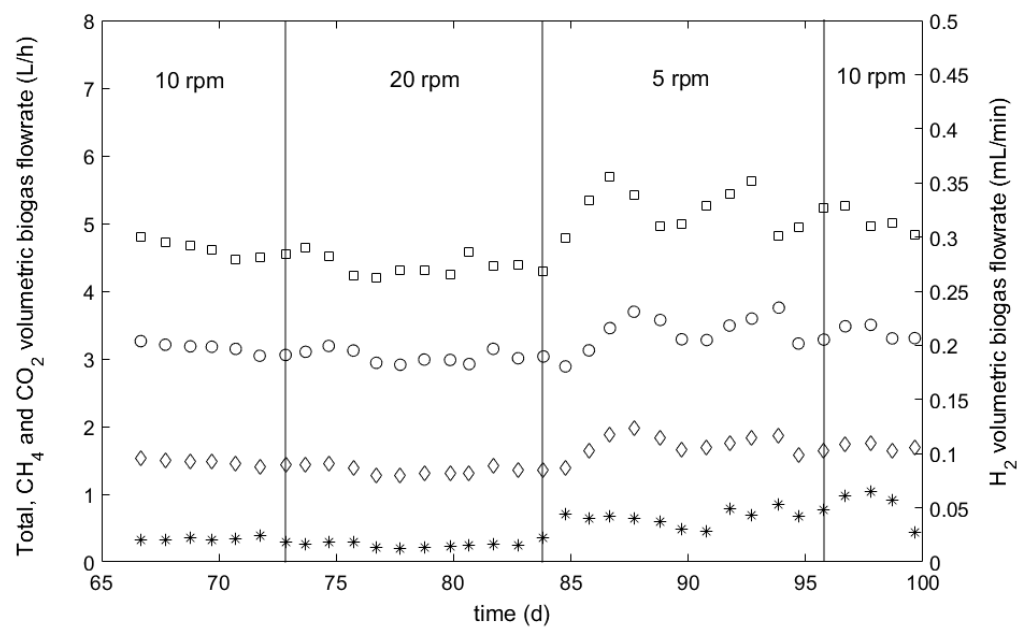


Figure 5: Impact of agitation rate on the total (\square), CO₂ (\diamond), H₂ (*) and CH₄ (\circ) volumetric flowrates.

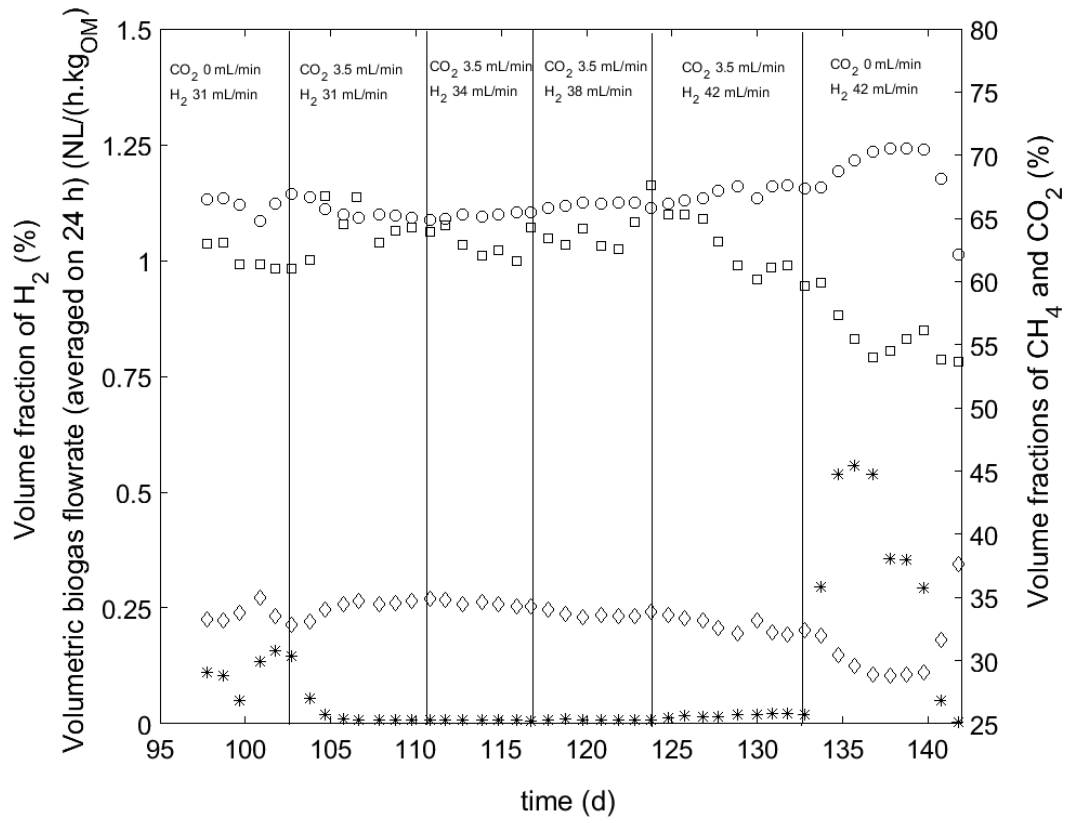


Figure 6: Impact of CO_2+H_2 gas on the CO_2 (\diamond), H_2 (*) and CH_4 (\circ) biogas composition and total biogas volumetric flowrate (\square).